Jour. of the KGS, Vol. 21, No. 2. March 2005, pp. 85~91

P-S Characteristics for End-bearing Pile in Granular Material

사질토 지반에서 선단지지말뚝의 P-S 특성

Lee, Yong-Joo[1] 이 용 주

요 지

본 논문에서는 실내모형실험 및 유한요소 프로그램인 CRISP을 이용하여 사질토 지반에 근입되어있는 선단지지 말뚝의 하중-침하(P-S) 관계를 규명하였다. 선단지지말뚝의 효과를 유한요소 해석에서 모사하기 위하여 몇 가지 형태의 인터페이스 요소들(slip elements)을 말뚝 주변 및 선단에 도입하였다. 비관련 소성흐름 법칙의 정도, 즉 지반강도 정수인 내부마찰각과 팽창각의 차이 정도를 고려한 Mohr-Coulomb 지반 모델에 있어서, 인터페이스 요소들이 포함된 선단지지말뚝은 내부마찰각과 팽창각의 차이가 유한요소 해의 수렴에 매우 중요한 역할을 하는 것으로 나타났다. 한편, 이와는 대조적으로 말뚝 주변에 적용한 인터페이스 요소 대신 Roller로 모사된 선단지지말뚝의 유한요소 해는 비관련 소성흐름 법칙의 정도에 대해서 영향을 받지 않고 수렴되는 것으로 나타났다.

Abstract

This paper investigates P-S (load-settlement) relationship for the end-bearing pile in granular material using the CRISP FE program with the laboratory 2D model pile load test. In order to simulate the effect of end-bearing pile problem in the FEA, the author adopts several forms of slip element around the pile length and the pile tip. Through this study it was found that the degree of non-associated plastic flow rule incorporated into the Mohr-Coulomb model for the end-bearing pile with the slip elements was a dominant factor in terms of numerical solution convergence. In contrast, the roller boundary used along the pile shaft showed a smooth convergence with respect to the degree of non-associated plastic flow rule.

Keywords : End-bearing pile, FEA, Slip element, Model test, Non-associated plastic flow rule, P-S

1. Introduction

The choice of flow rule controls the dilatancy effects, which in turn influence the volume changes. Volume change and shear strain modify the stress distribution and hence the strength mobilised. One small change produces a compound influence (Zienkiewicz et al., 1975; De Borst and Vermeer, 1984; Lee and Bassett, 2003). This is also a problem with real soil in which the dilatancy is extremely complex and is influenced by the stress path direction. Piling represents a rapidly increasing local stress "p" (s') below the pile tip and dilatancy is heavily suppressed. In the numerical simulation, the choice of dilatancy angle is, therefore, a key factor and will affect the convergence at the ultimate load when analysed with the "New Mohr-Coulomb" linear elastic-perfectly plastic soil model in CRISP package.

The author investigated the influence of the degree of non-associated flow expressed as the relationship between ϕ', the angle of shearing resistance and ψ, the angle of

1 Member, Senior Researcher, Track Geotechnology Research Group, Track & Civil Engrg. Research Department, KRRI (ucesyjl@hotmail.com)

dilatancy, which can be incorporated into the New Mohr-Coulomb soil model. Validation of the new M-C model was reported by the CRISP consortium Ltd at South Bank University (see "validation report" in CRISP consortium web-site). Several solution strategies are available to deal with the New M-C model. In this study, the FNR (full Newton-Raphson) solution scheme was adopted to solve the large displacement pile problem.

The author uses the "Single convergence" term when the result is based only on the displacement norm (Amir, 1998a) and "Double convergence" when based on both the displacement and the force norms. The convergence criteria for the double convergence under FNR (full Newton-Raphson), have recently been fully implemented in CRISP. The tolerance criteria was set to a value of 0.05 (5%) for this study. The author found that this value proved appropriate for the large displacement pile analysis, even though this value is somewhat higher than the 1-2% adopted by Potts et al. (1999). Pile loading was applied on the centre node point at the pile head. This replicated the centrally placed loading carried out in the physical model and the corresponding point at which deflections were also measured. The numerical pile loading simulation was performed by "DCM" (displacement control method) rather than "LCM" (load control method).

2. 2D Model Pile Load Test

The author carried out two dimensional model pile load test using a multiple sized aluminium rod mixture. The author's aluminium rod mixture contained six different diameters (viz. 2 mm, 3 mm, 6 mm, 9 mm, 12 mm and 20 mm) all 75 mm in length. It represented a well graded, idealised two dimensional granular material. The same batch of aluminium rods were used throughout the model tests. More details of the aluminium rod can be found in Lee (2004). In the model pile load test, both LCM (load control method) using the weights and DCM (displacement control method) using the screw jack were adopted to identify the P-S relationship, as shown in Fig. 1.

It should be noted that the reflective silver markers around the pile were only used for measuring the soil deformation patterns in terms of the close range photogrammetry. Consequently, these measured soil deformation patterns were led to the author's failure mechanism study (Lee, 2004). In this study, the author extracted the P-S (load-settlement) data for the comparison with FE P-S data.

3. Slip Elements

There is a very complex interaction between structures such as piles, retaining walls, tunnels and buried pipes

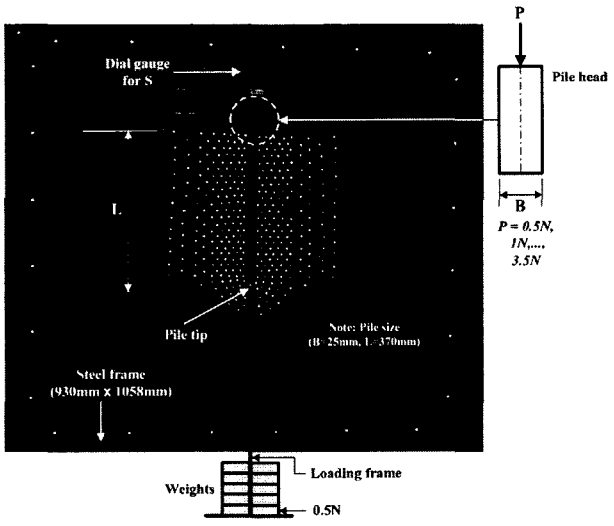

(a) LCM

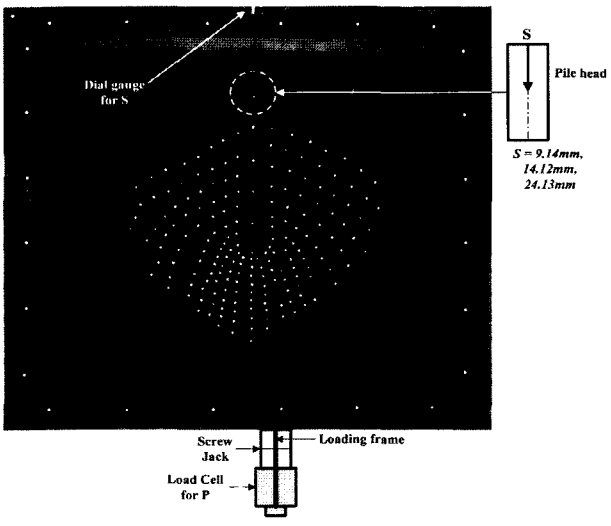

(b) DCM

Fig. 1. 2D model pile loading tests (LCM and DCM)

and the soil structure in which they are constructed. In finite element analyses, it is not only necessary to numerically model the structure and the surrounding ground but to carefully identify and choose properties for the interaction between them. This includes not only the obvious wall sides and pile vertical surfaces but also the underside of a wall or the pile base. Many methods have been proposed to model this complex interface behaviour in the finite element method (Lee, 2004).

Goodman et al. (1968) provide the concepts for the interface elements currently installed in the CRISP program. These allow slip to occur between dissimilar materials or materials having a large difference in their stiffness (Amir, 1998b). There is a constraint that a line of slip elements must be continuous between boundaries. Therefore, in order to simulate a dominant end bearing pile (where the base is frictionally fixed to the soil), two types of the slip element had to be used to maintain the continuity. Both were in theory of "zero" thickness but within the numerical format a nominal or fictitious thickness has to be used. On the pile sides the type I element has the slip characteristics (c=0.005 kPa and δ_w=5°). The type II element for the base which transmits both normal and shear forces, has the same characteristics as the soil ($\phi'=\delta_w$ =23° and c=0.1 kPa). The Mohr-Coulomb yield criterion was adopted by the author for both his slip elements to initiate slip. If the current shear stress (τ) exceeded the shear strength calculated from the normal stress with the standard relationship: $\tau_{limited}=c+\sigma_n tan\delta_w$ then slip occurs

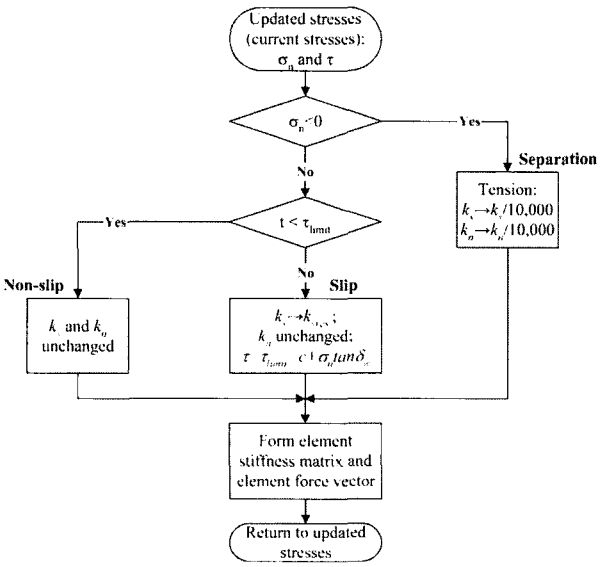

Fig. 2. Calculation procedures for slip element in the CRISP FE program

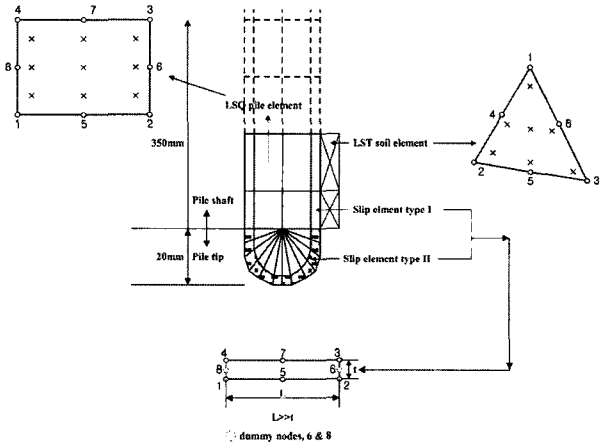

Fig. 3. Finite element types (LCM and DCM)

Table 1. Material parameters used in the FEA

Material	c′ (kPa)	ν	ϕ′ (°)	ψ (°)	E_0 (MPa)	m_E* (MPa/m)	m_c* (MPa/m)	γ_{bulk}	K_0
Pile	–	0.2	–	–	15500	–	–	23	–
Granular soil	0.1	0.35	23	0~23	1.6	10	0	24	0.66

Note: * based on the Gibson's soil.

Table 2. Slip element properties used in the FEA

Types	δ_w (°)	c (kPa)	k_n (MPa)	k_s (MPa)	k_{sres} (MPa)	t (m)
I	5	0.005	12839.5	2963	2.963	0.02
II	23	0.1	12839.5	2963	2.963	0.02
III	13	0.1	12839.5	2963	2.963	0.02

Note that δ_w: interface friction angle; c: interface cohesion; k_n: normal stiffness; k_s: shear stiffness; k_{sres}: residual shear stiffness; t: thickness.

and the residual shear stiffness (k_{sres}) is then used in the calculation of element stiffness. Checks are also determined if the element has gone into tension. The normal stiffness (k_n) and the shear stiffness (k_s) are set to 1/10000 of the compression stiffness (see Fig. 2).

Fig. 3 shows finite element types for the pile (linear strain triangle-LST), soil (linear strain quadratic-LSQ) and the slip element (two dummy nodes on the short side).

The Mohr-Coulomb model with non-associated flow rule requires five parameters. Three of these (viz. c′, ϕ' and ψ) govern the plastic behaviour, and the remaining two (E and ν) control the elastic behaviour. If associated flow conditions are assumed, the number of parameters reduces to four, as $\phi'=\psi$. The basic parameters are summarised in Table 1. It is noted that an isotropic elastic model was used for the pile.

The slip element properties are summarised in Table 2. The author experienced that the slip element parameters are very sensitive to the FE solution convergence, particularly, k_n and k_s values. These values should be higher than that for soil but lower than that for pile. If those values do not satisfy the above condition, numerical problems may occur (e.g. convergence and ill-conditioning).

4. Results

4.1 Identification of Degree of Non-associated Flow with or Without Slip Elements

The double convergence check in the CRISP provides reliable and accurate numerical solutions in terms of both stress and strain fields. The author has carried out a number of numerical runs with three different mesh conditions shown in Fig. 4 and with various values of ϕ' and ψ.

It should be noted that the half mesh on the pile centre was not used as it was required to mimic the physical test apparatus where (a) the model pile was not in the centre of the test frame and (b) the mesh was to be adopted later for the model tunnel set to one side of the centre of the mesh.

One set, with a constant ϕ' (23°), is shown in Figure

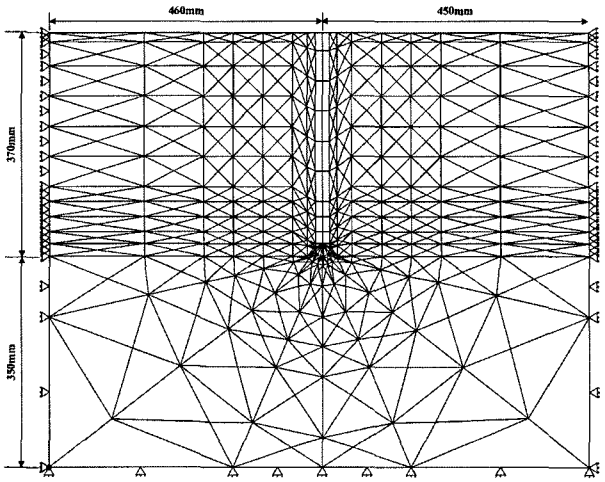

(a) Mesh A with type I and II slip elements (510 nodes and 934 elements)

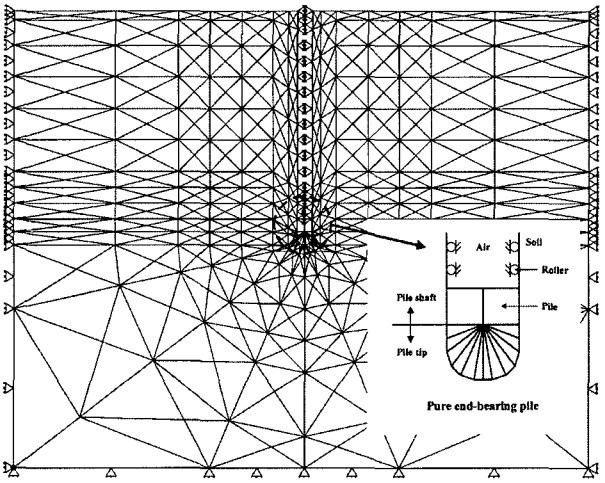

(b) Mesh A* with roller boundary along pile shaft (464 nodes and 872 elements)

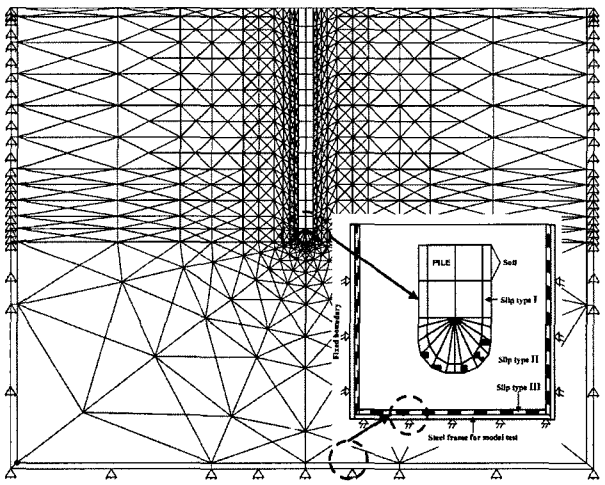

(c) Super mesh A with type I, II and III slip elements (911 nodes and 1704 elements)

Fig. 4. Three different mesh conditions for the end-bearing pile analysis

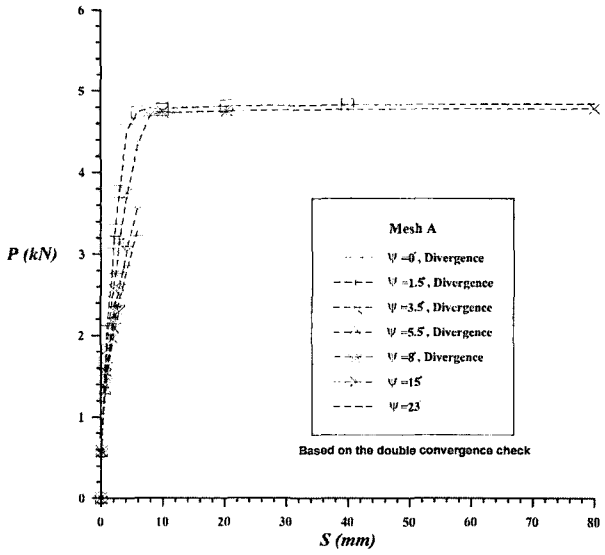

(a) P-S curves for Mesh A with ϕ'=23° (CPU time: 7 hrs)

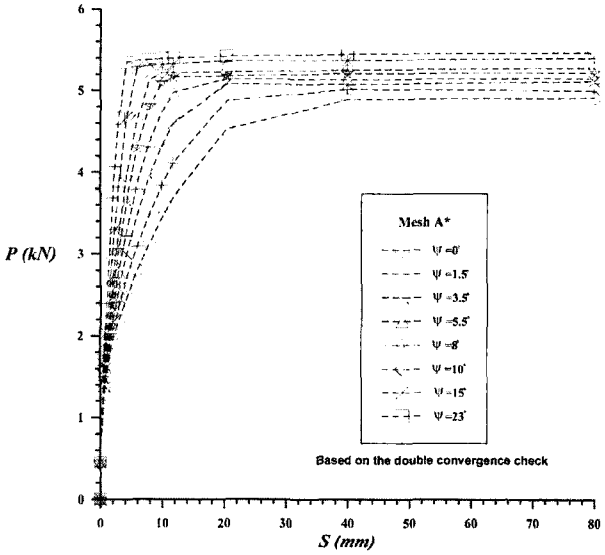

(b) P-S curves for Mesh A* with ϕ'=23° (CPU time: 1hr)

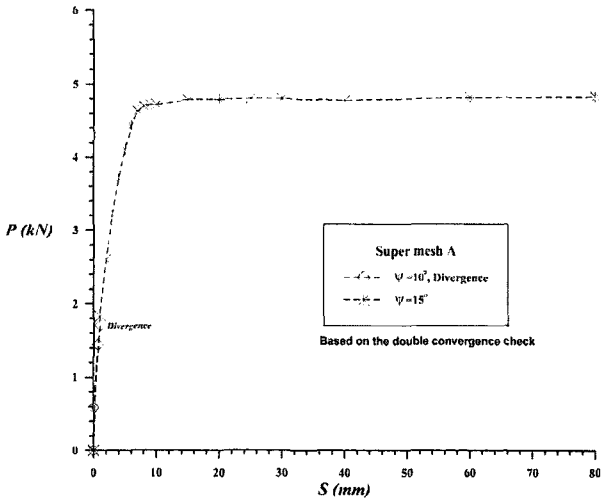

(c) P-S curves for Super mesh A with ϕ'=23° (CPU time: 2 days)

Fig. 5. P-S curves for the three different mesh conditions

5. Convergence breaks down under various conditions which vary with the mesh and with the difference between ϕ' and ψ.

The degree of non-associated flow rule incorporated into the Mohr-Coulomb model for the end-bearing pile with the slip elements was a dominant factor in terms of numerical solution convergence. In contrast, the roller boundary used along the pile shaft shows a smooth convergence with respect to the degree of non-associated flow rule.

Potts et al. (2001) have apparently succeeded in this problem with ψ down to zero. The author could not achieve this condition with slip elements. The difference in the ability to achieve convergence with a very high degree of non-associated flow between the author's study and Potts et al. (2001) is thought to be due in part to the following reasons: (a) the FNR technique used differs from the one used by Potts et al. (1999). Potts adopted the sub-stepping stress point algorithm rather than the return stress point algorithm in the CRISP; (b) the number of solution increments allowed; (c) some different boundary conditions; (d) the K_0 values adopted. Potts et al. (2001) start from an isotropic condition; the presenter due to the requirement to replicate a physical model under standard gravity conditions with ε_x=0 adopts the K_0 condition ($K_0 \cong 1-\sin\phi'$); (e) Finite element types. The author's experience with the CRISP program using FNR is that it is extremely difficult to satisfy the convergence unless the increment size is very small (i.e. as many increments as possible) although Potts et al. (1999) concluded that FNR results are insensitive to the increment size.

4.2 Comparison with the Model Pile Load Test

Fig. 6 shows the comparison of P-S curves with the model pile load test result. Mesh A* shows somewhat higher ultimate pile load (5.4 kN/m) but both Mesh A and Super mesh A approach the same ultimate pile load (4.75 kN/m) at S=10 mm. P-S data from the model load tests (LCM and DCM) show a good agreement with Mesh A and Super mesh A, particularly, zones for the elastic (between S=0 and S=4 mm) and the plastic (after S=21

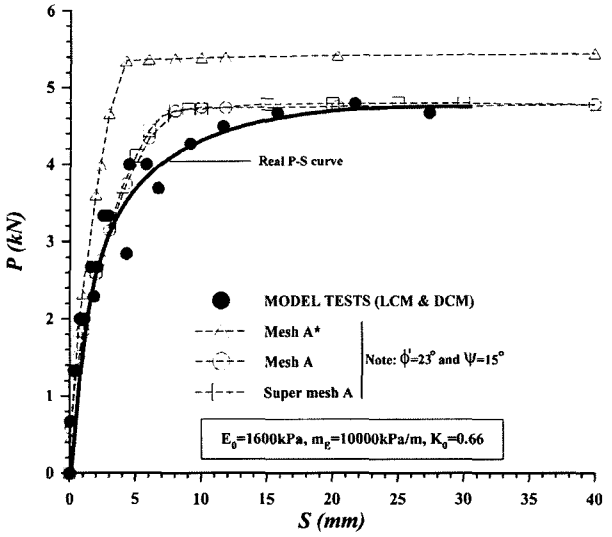

Fig. 6. Comparison with the model pile load test data in granular material

mm). However, the actual model data is similar to the hyperbolic pattern rather than the linear elastic-perfectly plastic assumed in the Mohr-Coulomb model. In a pile design point of view, the ultimate pile load is very important to decide the pile working load considering the safety factor.

4.3 Investigation of Boundary Conditions

Conventional FE programming sets remote lateral boundaries to a "far field" condition by expanding the dimensions of the more remote elements of the mesh and providing one direction of fixity with suitable "roller". Careful shear box tests conducted on the surface between the rod material and an aluminium plate provide a surface friction characteristic angle (δ_w or δ_{wall}) of 13°. The "roller boundaries" were therefore rather a poor representation of the real physical conditions at the real boundaries. These boundaries were located at a finite dimension from the pile and were directly replicated in the FE mesh (pile length, 370 mm; boundary distance left and right, 460 mm and 450 mm respectively). The author therefore modified mesh A to provide a "Super mesh A" in which rollers on the apparatus boundaries were replaced by a slip element type III. This had properties identical to type II slip elements except that ϕ' was replaced by δ_w, set to 13° and c=0.1 kPa. The inclusion of type III slip elements at the physical

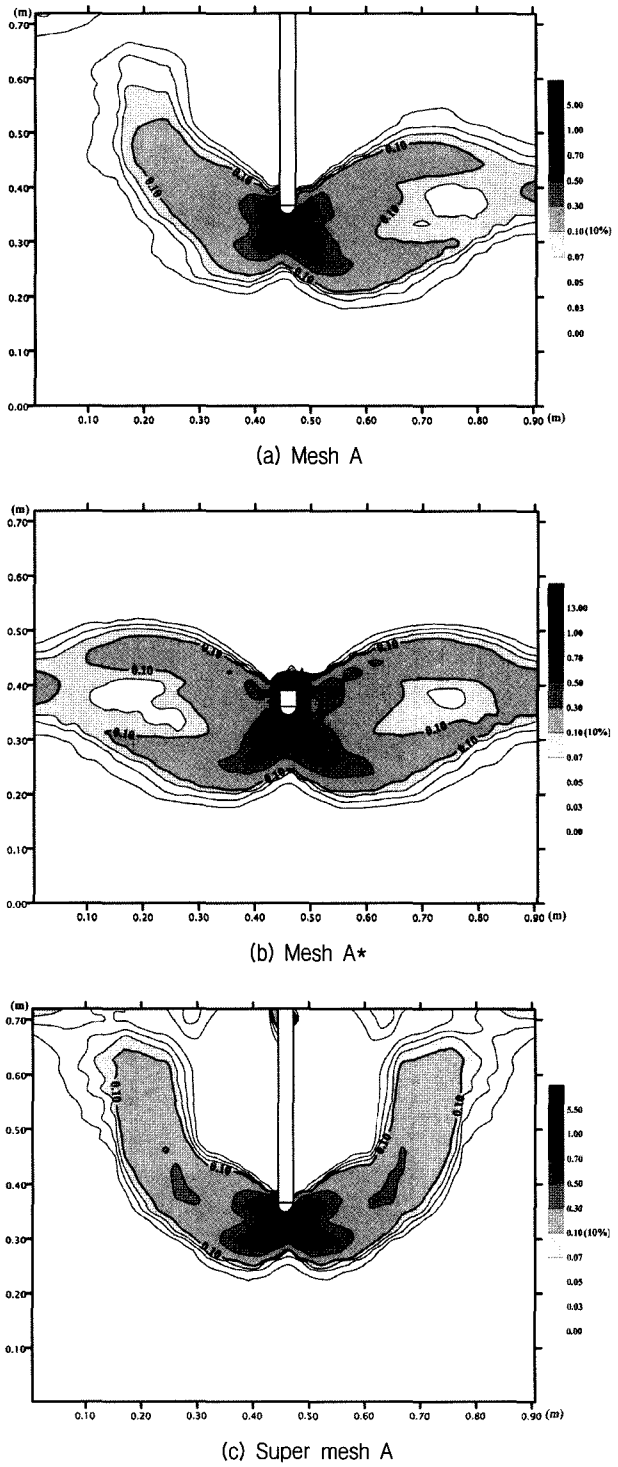

Fig. 7. Maximum shear strain contours at S=40mm (φ'=23° and ψ=15°)

boundaries radically changed the outer parts of the eventual shear mechanisms, as shown in Figure 7.

5. Conclusions

In order to satisfy the numerical convergence criteria

using slip elements, the difference between ϕ' and ψ was found to be restricted to between 10° and 13°. However, using the roller boundary in place of all the slip elements, the results were independent of the degree of non-associated flow, and consequently the double numerical convergence was achieved to ψ=0. The best replication of the author's physical model pile tests was achieved using the slip element type III replicating the physical properties between the side walls and the granular material. However, the CPU time was two days. This was unacceptable for multiple runs and the types I and II slip element system with lateral roller boundaries was accepted as a compromise.

Acknowledgments

This study is a part of the author's PhD study. The author appreciates to Reader Richard Bassett in the Department of Civil and Environmental Engineering at University College London, who has currently retired, for his invaluable discussion and encouragement in the author's PhD study.

References

1. Amir, R. (1998a), "The significance of non-associated plasticity", *Crisp News*, Issue No.6, November 1998.
2. Amir, R. (1998b), *Joint interface (slip) elements in CRISP in 2D and 3D space*, CRISP development report.
3. De Borst, R. and Vermeer, P. A. (1984), "Possibilities and limitations of finite elements for limit analysis", *Geotechnique*, Vol.34, No.2, pp.199-210.
4. Goodman, R. E., Taylor, R. L., and Brekke, T. L. (1968), "A model for the mechanics of jointed rock", *Journal of the Soil Mechanics and Foundations Division*, ASCE, SM3, pp.637-659.
5. Lee, Y. J. (2004), Tunnelling adjacent to a row of loaded piles, PhD Thesis, University College London, University of London.
6. Lee, Y. J. and Bassett, R. H. (2003), "End-bearing pile problem in granular material", *16th Crisp User Group Meeting*, London, South Bank University.
7. Potts, D. M. and Zdravković, L. (1999), *Finite element analysis in geotechnical engineering-Theory*, Thomas Telford, London.
8. Potts, D. M. and Zdravković, L. (2001), *Finite element analysis in geotechnical engineering-Application. Thomas Telford*, London.
9. Zienkiewicz, O. C., Humpheson, C., and Lewis, R. W. (1975), "Associated and non-associated visco-plasticity and plasticity in soil mechanics", *Geotechnique*, Vol.25, No.4, pp.671-689.

(received on Feb. 2, 2005, accepted on Mar. 27, 2005)